JOURNAL OF SCIENCE TECHNOLOGY AND EDUCATION 13(3), SEPTEMBER, 2025
E-ISSN: 3093-0898, PRINT ISSN: 2277-0011; Journal homepage: www.atbuftejoste.com.ng

Development of a Distributed Energy-Aware Position Algorithm for Flying Ad-Hoc Network

[1]Emmanuel K. Akut, [2]Aliyu D. Usman, [3]Kabir A. Abubilal, [4]Habeeb Bello, [5]Ahmed T., [6]John A. Bala, [7]Unite A. Dogo, [8]Augustine Zakka, [9]Ezekiel Agbon
[1,2,4,5,6,7,8&9]*Department of Electrical and Electronics Engineering, University of Jos*
[3]*Department of Electronics and Telecommunications Engineering, ABU Zaria*

ABSTRACT
The operational efficiency of FANET surveying a specific region is affected by the nature of the UAV's node placement, routing protocol, energy-aware task distribution, and node interaction amongst others. In this paper, three drones viz: Drone -1 (D-1), Master Drone (DM), and Drone 1 (D1) surveyed as FANET with DM aggregating packets from D-1 and D1 and communicating with the Static Ground Control Station (SGCS). The initial energy level of the drones' batteries was assumed to be 95% to 100% full prior to take-off. The energy consumed by a flying drone is calculated using drag, lift, and transmitting/receiving energy usage. For the node exchange technique, a number of events that covered the surveillance distance were 350. The first swapping command is triggered when the DM depletes 40% of its energy, followed by a second swapping command upon an additional 20% energy loss. To mitigate the risk of UAV failure resulting from energy depletion during surveillance, the mission was aborted, and all three UAVs initiated a return-to-base protocol once the energy level of the UAV functioning as the DM reached or dropped below the designated edge energy level. 796.134 J was obtained as threshold energy. Results obtained for the throughput, end-to-end delay, and Packet Delivery Ratio was 0.2343 Mbps, 0.009 x 10-3 sec, and 88.76% respectively. The developed model supports energy-aware and position of the UAVs during surveillance. It provides a dynamic UAV node placement for pipeline surveillance and interaction-based task distribution for cooperative task sharing between the UAVs and SGCS.

ARTICLE INFO
Article History
Received: April, 2025
Received in revised form: May, 2025
Accepted: June, 2025
Published online: September, 2025

KEYWORDS
UAV, Energy-Aware, Positioning, Through-Put, Delay

INTRODUCTION

The significant role play by Pipelines in oil and gas industries cannot be over emphasized (Ding *et al.*, 2018). These comprise the provision of an inexpensive as well as quicker mode in conveying finished and unfinished products. Notwithstanding, these pipelines sometimes rupture due to forces acting from both inside and outside and the activities of vandals etc. These, as a results, introduce ecological toxic waste, interference to water ways, imbalance ecosystem etc. (Shrit *et al.*, 2018).

Due to their numerous applications in both civil and military task, researchers are shifting their attention to the use of UAVs since their influx in the 19th century (Fiedler, 2016) and (Benyeogor *et al.,* 2020). UAV technology is also use in the oil and gas productions, to replace the outmoded monitoring of pipelines using obsolete instruments by firm employees. If the surveillance region is wide and several drones are to patrol as a team, a lead UAV known as Master Drone's (D_M) communicates with other UAVs and the ground station (Antonio *et al.,* 2021).

Corresponding author: Emmanuel K. Akut
akute@unijos.edu.ng
Department of Electrical and Electronics Engineering, University of Jos.

JOURNAL OF SCIENCE TECHNOLOGY AND EDUCATION 13(3), SEPTEMBER, 2025
E-ISSN: 3093-0898, PRINT ISSN: 2277-0011; Journal homepage: www.atbuftejoste.com.ng

Since UAV's energy is limited, scholars have been working on prolonging the UAV's flight time. These include improving the battery quality, battery charging techniques, payload optimization etc. the proposals are effective but also, on a high cost. Moreover, there is need to monitor D_M's energy lost as a result of data dissemination and to switch D_M with the drone holding greater energy when the D_M's vigor falls below threshold (Akut *et al*., 2023) and (Kochetkova, 2018). This will include how the UAVs broadcast their movement status to the Master Drone (Santos *et al*., 2021). To avoid excess loss of energy due to information dissemination and data aggregation, there is need for a communication scheme for nodes and SGCS (Antonio *et al.,* 2021).

Routing protocol defined as prescribed policies governing communication among nodes in a network (Shukla *et al.*, 2016). They are fundamental to U2U communication, as they critically influence the reliability and efficiency of delivery (Hu *et al.*, 2020). UAV flight time is constrained by various energy-consuming factors, including payload, net weight, data handling, task scheduling, and control systems. As most UAVs rely solely on battery power, manufacturers work to optimize these elements, yet energy limitations persist. This paper proposes algorithms to optimize UAV placement for coverage, manage UAV–SGCS communication, enable energy-aware messaging, and coordinate task distribution among UAVs. (Ullah, S. *et al*., 2022).

METHOD

Conceptualization of the network is made up of numerous UAVs from D_{-1} to D_{-N} on the left of D_M and D_1 to D_N on the right side will be placed over the surveillance area. Though three drones were used for this research i.e. D_{-1}, D_M and D_1, standard petroleum pipeline is used for the surveillance space. Every one of the drones is to survey a segment of the pipe area over a height of *h* meters. The choice of *h* meters height will be made to create a scenario with a better vision positioning system and to avoid obstacles from tall buildings and trees (Akut *et al*., 2023). While on a surveillance mission, D_M will have the capacity to swap with other drones in the FANET base on energy-aware shared information.

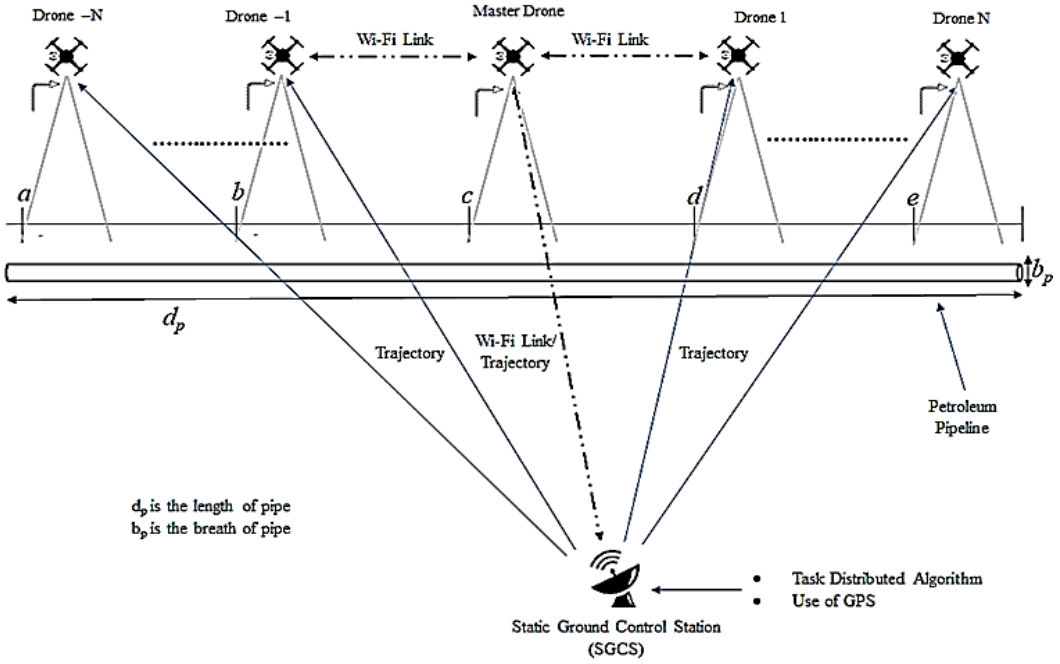

Fig. 1: Research conceptual model

Corresponding author: Emmanuel K. Akut
akute@unijos.edu.ng
Department of Electrical and Electronics Engineering, University of Jos.

JOURNAL OF SCIENCE TECHNOLOGY AND EDUCATION 13(3), SEPTEMBER, 2025
E-ISSN: 3093-0898, PRINT ISSN: 2277-0011; Journal homepage: www.atbuftejoste.com.ng

The algorithm simulations were implemented in MATLAB R2021a, with the configuration parameters detailed in Table 1.

Drones Positioning

As presented in Fig. 1, before deployment, the drones' $\{D_{-1}, D_M, D_1\}$ initial positions are $\{(x_i^{-1}, h_i^{-1}), (x_i^M, h_i^M) \text{ and } (x_i^1, h_i^1)\}$ in the x–y plane. The drones' final deployment coordinates are specified as follows $\{(x_f^{-1}, h_f^{-1}), (x_f^M, h_f^M) \text{ and } (x_f^1, h_f^1)\}$ where h_f represents the drone's flight altitude and is defined by the following equation (Akut *et al.,* 2023):

$$h_f^j = \sum_{j=-N}^{N} \begin{cases} h_m & if\ h_f^j \geq 10 \\ h_f^j & if\ otherwise \end{cases} \quad (1)$$

Where h_f^j indicates altitude associated with drone j, h_m signifies extreme allowable flight altitude for the drones -N, through M to N.

Table 1: Configuration Parameters

S/N	Factor	Description	Rate
1	N_d	Number of drones	3
2	I	Battery rating of the drone	1100 mAh
3	V	Battery voltage	3.8 V
4	H*L*B	Dimension of the drone	(98 x 92.5 x 41) mm
5	K	Scaling factor for changing mAh to A	3.6
6	E	Battery capacity of the drone	15.048 kJ
7	it	Total number of events	300/350
8	d_p	Length of the pipeline	12.2 m
9	b_p	Diameter of the pipeline	1.22 m
10	v_{D_j}	Drone's velocity	4 m/s
11	θ	Observation angle of the drone	82.2^0
12	h_m	Define the drone's flight altitude	10 m

Static Ground Control Station Placement (SGCS)

The drones were lunch from SGCS to the initial surveillance region using Eqns (2) to (4), the navigational paths and pairwise distances among drones and SGCS, lunch flight time and duration were calculated as follow:

$$d_x D_j = \left(\frac{\left(d_y D_j - C_{x=0} D_j \right)}{h_f} \right) \left(x_f - x_i \right) \quad (2)$$

$$E_{D_j} = \sqrt{\left| h_{fD_j}^2 \right| + \left| x_{fD_j}^2 - x_{iD_j}^2 \right|}\ m \quad (3)$$

$$T_{D_j}\left(h_f \right) = \frac{E_{D_j}}{v_{D_j}} = \frac{\sqrt{h_{fD_j}^2 + \left| x_{fD_j}^2 - x_{iD_j}^2 \right|}}{v_{D_j}} s \quad (4)$$

Where d_x denotes the instant location of drone *i*along the x-axis during the placement phase. (*j* = -1, M and 1), d_y Denotes the instant y-axis location of the drone during the placement phase,

Corresponding author: Emmanuel K. Akut
akute@unijos.edu.ng
Department of Electrical and Electronics Engineering, University of Jos.

JOURNAL OF SCIENCE TECHNOLOGY AND EDUCATION 13(3), SEPTEMBER, 2025
E-ISSN: 3093-0898, PRINT ISSN: 2277-0011; Journal homepage: www.atbuftejoste.com.ng

h_f corresponds to the last flight altitude, h_i corresponds to the early flight altitude,

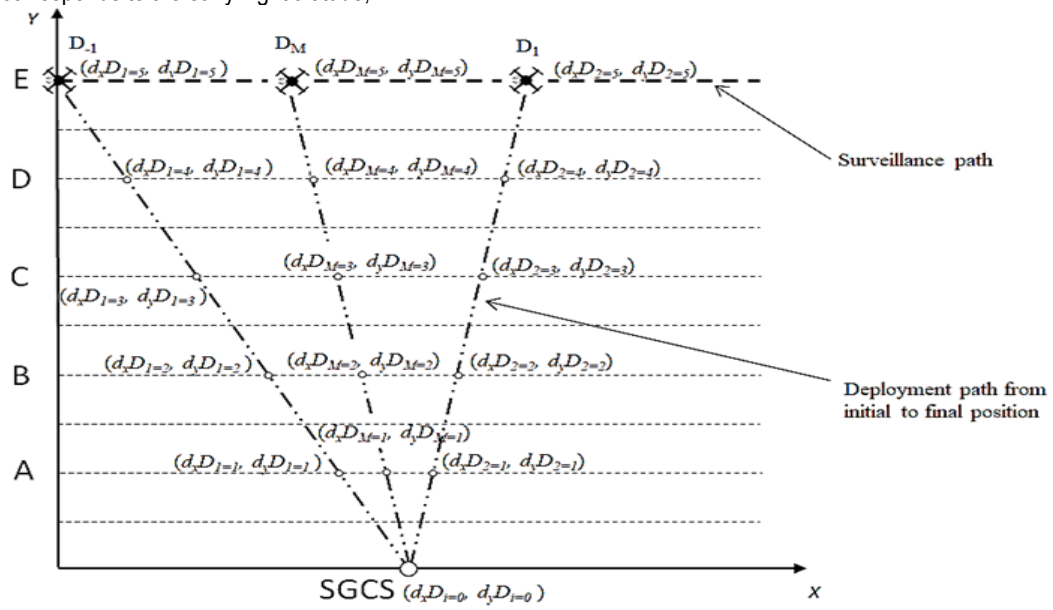

Fig. 2: Drones' Trajectories during Deployments

x_f marks the end-stage UAV location on x-coordinate, x_i defines the initial horizontal coordinate of the UAV, $c_{x=0}$ Corresponds to the coefficient governing collision mitigation during UAV activity in the surveillance zone, E_{D_j} is the Euclidean distance and $T_{D_j}\left(h_f\right)$ represents the lunch flight time (Fernandez *et al*., 2020). The drones' deployment trajectories acquired using equation (4) is as depicted in Fig. 2 where points A, B, C, D and E were selected for the drones to broadcast their GPS positions, energy level and speed along the trajectories.

Communication Scheme for Node Formation and SGCS

The communication between the drones and the SCGS is divided into time notches, with "n" determining each period. In the resulting schedule, each drone must have one transmission notch. The SCGS is assumed to have full control of the orientation and position of individual drones. Each drone is equipped with a radio for connectivity with the SCGS via D_M and is aware of its location through GPS.

Energy-Based Leader Drone Determination Mechanism

To ensure energy-efficient implementation of the surveillance mission, each UAV must maintain a preliminary battery state-of-charge (SoC) within the range of 95% to 100% of its full energy capacity that is, 15.048 kJ. For simulation purposes, the initial battery energy levels of the UAVs were modeled and initialized based on the formulation provided in Eq (5):

$$E_{d_j}(\Xi_{\min},\Xi_{\max},N_d)=\Xi_{\min}+\Theta(N_d,1)\times(\Xi_{\max}-\Xi_{\min}) \quad (5)$$

Here $\Xi_{\max}$ & $\Xi_{\min}$ describes the drones' energy capacity bounds, N_d denotes the cumulative count of drones in the system, and Θ, a normally distributed variable, introduces stochasticity into the initialization of E_d. UAV D_{-1} is assigned higher initial energy than D_1 to reflect non-uniform energy distribution.

Corresponding author: Emmanuel K. Akut
akute@unijos.edu.ng
Department of Electrical and Electronics Engineering, University of Jos.

JOURNAL OF SCIENCE TECHNOLOGY AND EDUCATION 13(3), SEPTEMBER, 2025
E-ISSN: 3093-0898, PRINT ISSN: 2277-0011; Journal homepage: www.atbuftejoste.com.ng

Node Exchange Technique

UAV energy dissipation occurs during vertical ascent, hovering, horizontal flight, and communication tasks such as transmission, reception, and data aggregation (Aiello et al., 2021). Post-takeoff, energy decreases due to aerodynamic drag, gravitational forces, and communication overhead. The UAV's instantaneous energy at time t during surveillance is given by (Akut *et al*., 2023):

$$cE_{D_M} = iE_{D_M} - \int_0^t P_R(dt) - \int_0^t E_{agg}(dt) \quad (6)$$

Where iE_{D_M} denotes the master UAV's initial energy state at the commencement of the mission, P_R represents the power consumed during drone flight and E_{agg} is the power consumed in UAV-to-UAV and UAV-to-SGCS communication.

UAV Exchange

Given the rapid energy depletion of D_M, a handover to D_{-1} is triggered once D_M's initial energy is exhausted below 40%. This ensures that the initial master drone maximizes its surveillance coverage Prior to exceeding its defined energy limit. The secondary handover situation is triggered when the succeeding $D_{-1\text{-}N}$ (i.e. old D_M) acquired another loss of 20% of its battery capacity. Therefore, $D_{M\text{-}N}$ (old D_{-1}) interchange with D_1. The following expressions capture these conditions (Akut *et al*., 2023):

$$D_M = \begin{cases} D_M & if \ \ cE_{D_M} \geq 60\% \times iE_{D_M} \\ (Swap)\, D_M, D_{-1} & if \ \ cE_{D_M} < 60\% \times iE_{D_M} \end{cases} \quad (7)$$

where: D_{-1} represents UAV -1, iE_{D_M} refers to energy of D_M at mission onset while cE_{D_M} denotes the time-varying instantaneous energy of DM throughout the surveillance operation

$$D_{M-N} = \begin{cases} D_{M-N} & if \ \ 60\% \times iE_{D_M} > cE_{D_M} \geq 40\% \times iE_{D_M} \\ (Swap)\, D_{M-N}, D_1 & if \ \ cE_{D_M} < 40\% \times iE_{D_M} \end{cases} \quad (8)$$

here $D_{M\text{-}N}$ designates the newly elected master UAV, D_1 identifies Drone 1, iED_M denotes the initial energy allocation of the master UAV, and cED_M represents its instantaneous energy state at time t.

Tables 1 and 2 depict the deployment and energy-aware checking algorithms respectively. Three drones were used in the simulation therefore, -N and N represents -1 and 1 respectively.

Table 2: UAV Node Deployment Algorithm

Algorithm 1: UAV node deployment Algorithm

Input: $(x_i^{-N}, h_i^{-N}); (x_i^M, h_i^M); (x_i^N, h_i^N); \theta; d_p; b_p; V; I; K; E_{\min}; E_{\max}$

Output: $D_{-N}; D_M; D_N; (x_f^{-N}, h_f^{-N}); (x_f^M, h_f^M); (x_f^N, h_f^N);$

1. *Quantify the extent of the coverage area*
2. *Ascribe D_{-1}, D_M, D_1*
3. *Determine first UAV coordinates from provided parameters* $(x_i^{-N}, h_i^{-N}); (x_i^M, h_i^M)\ and\ (x_i^N, h_i^N)$
4. *Determine optimal UAV navigation*
5. *Evaluate the total path length for each UAV*
6. *Compute the transit duration per UAV*
7. *Establish the communication framework enabling node structuring and SGCS*
8. *If the UAV is located at its target waypoint*
9. ***|*** *Configure UAV as a communication node*
10. ***Else***
11. ***|*** *Loop back to Step 4 and re-execution*

Corresponding author: Emmanuel K. Akut
akute@unijos.edu.ng
Department of Electrical and Electronics Engineering, University of Jos.

JOURNAL OF SCIENCE TECHNOLOGY AND EDUCATION 13(3), SEPTEMBER, 2025
E-ISSN: 3093-0898, PRINT ISSN: 2277-0011; Journal homepage: www.atbuftejoste.com.ng

Algorithm 1: UAV node deployment Algorithm

12. **Output**: $D_{-N}; D_M; D_N; (x_f^{-N}, h_f^{-N}); (x_f^M, h_f^M); (x_f^N, h_f^N);$
13. ***Stop***

Performance Metrics

Throughput: The throughput, sometimes called the flow rate is the of bits of data packets successfully delivered to the destination node within a specified time interval, which can be written as (Khan *et al*, 2020):

$$T_{(r)} = \frac{T_p}{T} \quad (9)$$

where: $T_{(r)}$ represents the network throughput, T_p represents the cumulative number of packets count, T signifies the time taken to send the packets. As established in the literature, the signal received by the client undergoes gradual attenuation with increasing distance, reaching a threshold at the maximum communication range. A throughput distance relationship model can be used to express this (Pahlavan & Levesque, 2005):

$$T(r) = -0.1669d + 5.343 \quad (10)$$

where $T_{(r)}$ represents the throughput function and d denotes the spatial parameter.

Table 3: Energy-Aware Checking Algorithms

Algorithm 2: UAV Energy Level Assessment Algorithm

Input:

$\theta; d_p; b_p; V; I; K; E_{\min}; E_{\max}; a; b; £_d; \rho; A_d; S; m; g; r,$

$U = \{D_{-N}, D_M, D_N\}$

it = set of mission events for the entire UAV

iE_{D_M} *= starting state-of-charge (SoC) of* D_M

$< 50\% \times iE_{D_M}$ *= swapping energy threshold value*

$< 35\% \times iE_{D_M}$ *= second swapping energy threshold value*

RE_{thr} *= critical energy benchmark for base return manoeuvre*

Algorithm 2: UAV Energy Level Assessment Algorithm

Output: SL^{x_f} *: Update final position following UAV handover* U_j

1. *Designate* D_M *to the Master Drone*
2. *Assign initial UAV location following Methodology I*
3. ***While*** $cE_{D_M} > RE_{thr}$ **do***using* equation (9)
4. ***If*** D_M *energy is* $< 50\% \times iE_{D_M}$
5. *Swap UAV position and update status using equations (8)*
6. ***Else***
7. *Resume from Step 4*
8. ***End if***
9. *If the energy level of the master drone* $< 35\% \times iE_{D_M}$
10. *Drone positional exchange and status update using equations (7)*
11. ***Else***
12. *Resume from step 9*
13. ***End if***
14. ***End while***
15. ***Output***: SLx_f *: Update final position following UAV handover* U_j
16. ***End***

Transmission Delay: This is the delay induced by the link's data rate. The length of the packet determines this delay, which is independent of the distance between the two nodes. This delay is proportional to the packet length in bits and can be calculated as (Yang & Liu, 2019):

$$D_{(r)} = \frac{1}{n}\sum_{i=0}^{n-1}(P_i(T_r)P_i(T_s)) \quad (11)$$

where: $D_{(r)}$ represents the transmission delay in seconds, P_i is the *i*th packet, T_r denotes the reception timestamp of a packet, T_s signifies the

Corresponding author: Emmanuel K. Akut
akute@unijos.edu.ng
Department of Electrical and Electronics Engineering, University of Jos.

JOURNAL OF SCIENCE TECHNOLOGY AND EDUCATION 13(3), SEPTEMBER, 2025
E-ISSN: 3093-0898, PRINT ISSN: 2277-0011; Journal homepage: www.atbuftejoste.com.ng

corresponding transmission timestamp, and *n* is the total number of packets successfully delivered to the destination node

Packets Delivered Ratio: Packet Delivery Ratio (PDR) quantifies the proportion of successfully received packets at the destination node relative to the total number of packets transmitted by the source.

$$Packets\ Delivered\ Ratio = \frac{No.\ of\ \ packets\ delivered}{Total\ \ packets\ sent} \quad (12)$$

Many researchers reported on these performance metrics in a FANET, although no scenario used is similar to this novel research.

Node Deployment

Fig. 3 illustrates the flight trajectories of the three UAVs, with each line representing the path of an individual drone and the red, black, and green lines represent D_{-1}, D_M, and D_1 respectively. The dots (i.e. * * *) at a vertical interval of 2 m marks the locations at which the three UAVs transmit their telemetry data – comprising x-y coordinates, velocity vectors, energy levels, and orientation. The pipeline is located at 1.0 m along the y- coordinate, indicating its vertical displacement from ground level.

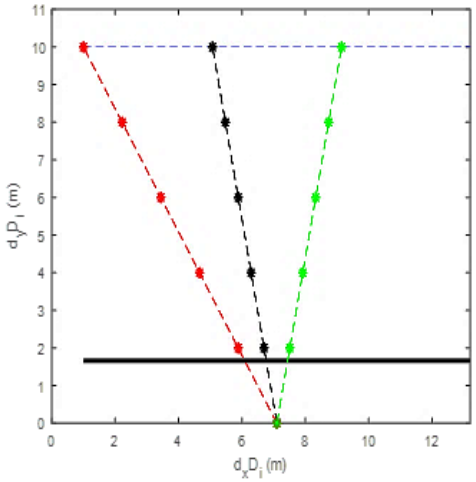

Fig. 3: Drones' Trajectories

Node Exchange Technique

The simulation was conducted to evaluate dual D_M handovers. The real-time energy state of D_M during the surveillance phase was quantified using Equation (6), incorporating the cumulative power expenditure attributed to multi-source data aggregation from two subordinate UAVs and sustained communication with the SGCS, D_M's energy depletes more rapidly than that of D_{-1} and D_1. Equations (7) and (8) govern the first and second handover events, respectively.

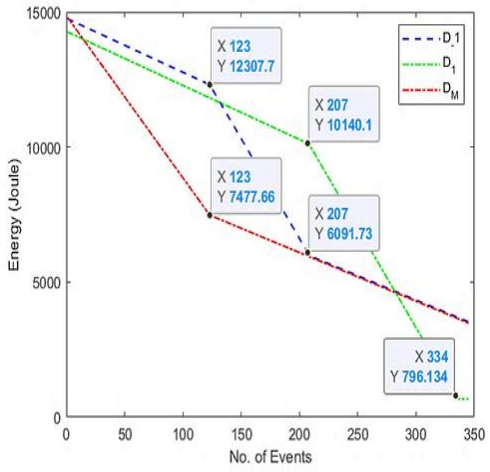

Fig. 4: Master Drone Swapping

Fig. 4 presents the simulation results, with the initial DM's energy serving as the reference. The first handover is triggered after a 40% energy loss, followed by a second handover after an additional 20% depletion.

During the simulation, the first master drone (D_M) handover occurred at an energy level of 7.477 kJ for D_M and 12.307 kJ for D_{-1}, corresponding to the 123rd event out of 350 scheduled mission events. The second handover was triggered at the 207th event when D_M's energy dropped to 6.091 kJ and D_1's energy was 10.140 kJ. During the 334th scheduled event, the active D_M attained its predefined return-to-base (RTB) energy benchmark. SGCS then issued an RTB command, prompting immediate mission termination and the return of all three UAVs to the base station.

Throughput

Corresponding author: Emmanuel K. Akut
akute@unijos.edu.ng
Department of Electrical and Electronics Engineering, University of Jos.

JOURNAL OF SCIENCE TECHNOLOGY AND EDUCATION 13(3), SEPTEMBER, 2025
E-ISSN: 3093-0898, PRINT ISSN: 2277-0011; Journal homepage: www.atbuftejoste.com.ng

As presented in subsection 2.7.1 and using equation (9), the results obtained from simulation for throughput is as presented in Fig. 5.

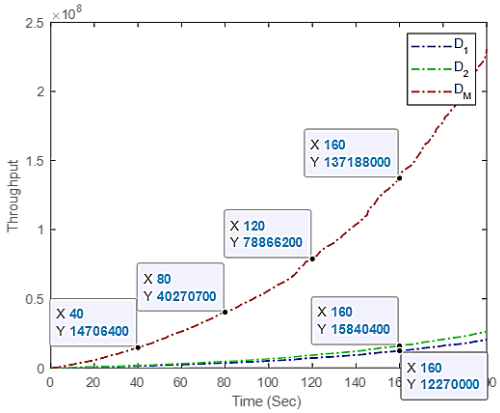

Fig. 5: Throughput of the Three UAVs with Time

Fig. 5 depicts the throughputs of the three UAVs, with D_{-1} having the least throughput and D_M with the highest. The graph shows cumulative throughput with time. The value of D_M's throughput at 40 s, 80 s, 120 s, and 160 s were 0.368 Mbps, 0.503 Mbps, 0.657 Mbps, and 0.857 Mbps respectively. The throughput slightly increases with time. This is due to the fast movement of the nodes and changing topology as the UAVs cover the surveillance space.

Transmission Delay

As presented in subsection 2.7.2, transmission E2E delay is the time difference between packet send time and packet delivery time. Using equation (11), the results obtained from simulation for transmission delay are as presented in Figs. 6 and 7.

As depicted in Fig. 6, the average time to send packet takes less than 0.5 ms to initiate, while the delivery time is slightly greater than the send time. The average E2E delay as obtained in this simulation is 0.009 ms. The variation in packets sent and delivery time as indicated in Fig. 6 is largely due to fast movement of the UAV nodes and changing topology.

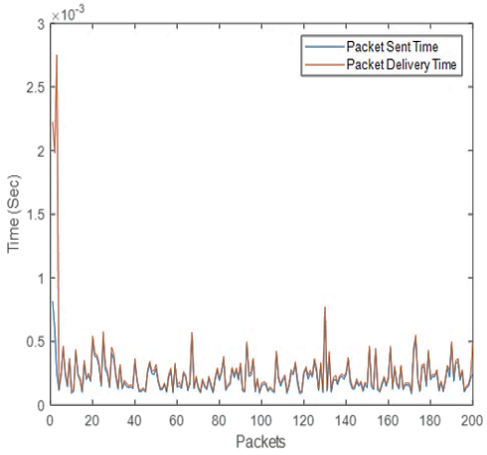

Fig. 6: E2E Transmission Delay

In Fig. 7, a segment of Figure 6 between 80th and 90th packets is reproduced to give a clearer picture. For the 82nd packet, the send and delivery time were 0.3552 ms and 0.3808 ms respectively, while the 85th packet send and delivery time were 0.1615 ms and 0.1757 ms respectively. The E2E delays for the 82nd and 85th packets were 0.0256 ms and 0.0142 ms respectively. From Fig. 7, it is obvious that the lesser the time to initiate send packet the lesser the delivery time. This time variations mainly depend on position and topology of the nodes as they move very fast.

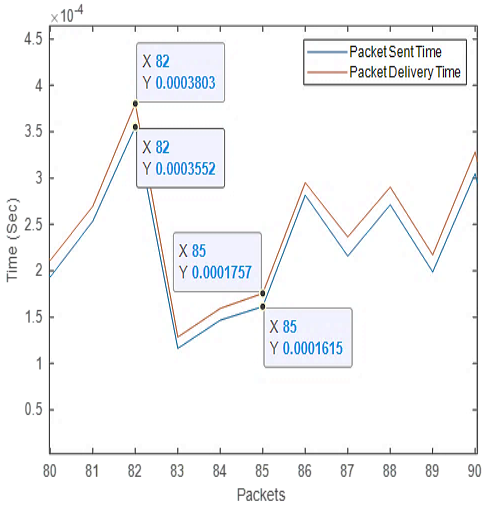

Fig. 7: 82nd and 85th E2E Transmission Delay

Corresponding author: Emmanuel K. Akut
akute@unijos.edu.ng
Department of Electrical and Electronics Engineering, University of Jos.

Packet Delivery Ratio (PDR)

PDR has been presented in subsection 2.7.3. It quantifies the ratio of successfully received packets at the destination node to the total number of packets transmitted by the source, serving as a metric for communication reliability. The results obtained from simulation for PDR are as presented in Fig. 8 using equation (12).

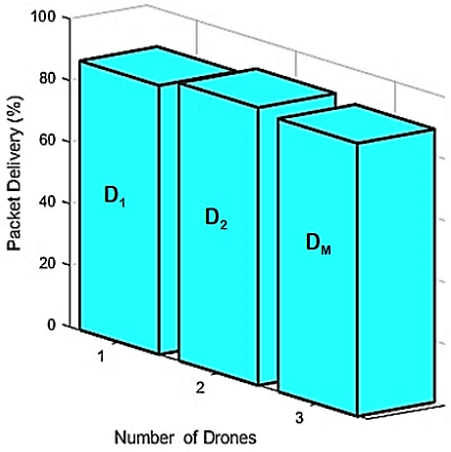

Fig. 8: Percentage of Packet Delivery

Fig. 8 depicts the PDR of the three UAVs in percentage. From the simulation display results, the PDR for D_{-1}, D_1, and D_M were 87.38%, 90.23%, and 88.66% respectively. The average PDR is 88.76%. The density of packets sent increases from D_1, D_{-1} to D_M, from the result, it is noticeable that the higher the density of packets sent, the lower the percentage PDR. Though, the average percentage PDR is significantly good.

CONCLUSION

This study presents a dynamic UAV node placement strategy for petroleum pipeline observation using a FANET architecture composed of three drones. The D_M maintained communication with the SGCS. Prior to deployment, UAV batteries were presumed to be charged to 95 – 100% of full capacity. The first D_M handover was initiated after 40% energy depletion, followed by a second handover at an additional 20% loss. Return-to-base (RTB) threshold energies were calculated for all UAVs, with the D_M's RTB threshold set at 796 J. Simulation results demonstrated effective node exchange by the proposed algorithms, enabling optimized energy utilization, extended surveillance duration, and cooperative task distribution. The evaluated performance metrics – namely end-to-end delay, throughput, and packet delivery ratio (PDR) – demonstrated the system's operational efficiency and communication reliability.

ACKNOWLEDGEMENT

This research work was funded by the Nigerian Tertiary Education Fund (TETFUND). ID: 032/IBR/UNIJOS.2024.

REFERENCES

Aiello, G., Inguanta, R., D'Angelo, G., Venticinque, M. (2021) Energy Consumption Model of Aerial Urban Logistic Infrastructures. *Energies 2021*, 14, 5998. https://doi.org/10.3390/en14185998

Akut E. K. et al., (2023) "Drone's node placement algorithm with routing protocols to enhance surveillance" Intl. Journal of Elect. and Compt. Engr. (IJECE). 13(4), pp 4194 – 4203. doi: 10.11591/ijece.v13i4.pp4194-4203

Akut E. K. et al., (2023) "Energy-aware Message Distribution Algorithm for Enhance FANET Pipeline Surveillance Reliability" Sci. African Elsevier Journal. 20(2023) e01660, pp 1 – 14. doi: 10.1016/j.sciaf.2023.e01660

Antonio, G., Ana-Maria, M., Juan-Carlos, S., Maria-Dolores, C. (2021). A Comparative Performance Evaluation of Routing Protocols for Flying Ad-Hoc Networks in Real Conditions. *Applied Science 2021*, 11, 4363. doi.org/10.3390/app11104363

Benyeogor, M., Olatunbosun, A. and Kumar, S. (2020). Airborne System for Pipeline Surveillance Using an Unmanned Aerial Vehicle. *European Journal of Engineering Research and Science. EJERS,* 5(2), 178-182

Corresponding author: Emmanuel K. Akut
akute@unijos.edu.ng
Department of Electrical and Electronics Engineering, University of Jos.

Ding, G., Wu, Q., Zhang, L., Lin, Y., Tsiftsis, T. A., & Yao, Y. D. (2018). An Amateur Drone Surveillance System Based on the Cognitive Internet of Things. *IEEE Communications Magazine,* 56(1), 29–35. doi:10.1109/mcom.2017.1700452

Fernandez, S. A., Carvalho, M. M. and Silva D. G. (2020). A Hybrid Metaheuristic Algorithm for the Efficient Placement of UAVs. *Algorithms 2020*, 13, 323; doi:10.3390/a13120323

Fiedler, J. (2016). *An Overview of Pipeline Leak Detection Technologies*. KROHNE, Inc. 7 Dearborn Road. Peabody, MA 01960. asgmt.com/wp-content/uploads/2016/02/04.pdf.

Hu, Y., Zhang, F., Tian, T., and Ma, D. (2020). Placement Optimisation Method for Multi-UAV Relay Communication. *IET Communication*, 14(6), 1005-1015 doi: 10.1049/iet-com.2019.0518

Khan, I. U., Qureshi, I. M., Aziz, M. A., Cheema, T. A. and Shah, S. B. H. (2020). Smart IoT Control-Based Nature Inspired Energy Efficient Routing Protocol for Flying Ad Hoc Network (FANET). *Special Section on Evolving Technologies in Energy Storage Systems for Energy Systems Applications.* Doi: 10.1109/ACCESS.2020.2981531

Kochetkova, L. I. (2018). Pipeline monitoring with unmanned aerial vehicles. *Journal of Physics: International Conference Series,* 1015, 042021. doi:10.1088/1742-6596/1015/4/042021

Pahlavan, K. & Levesque, A. H. (2005). *Wireless Information Networks* (2nd ed). John Wiley & Sons, 18-25.

Santos, G., Martins, J., Coelho, A., Fontes, H., Ricardo, M. and Campos, R. (2021). A Fast Gateway Placement Algorithm for Flying Networks. *2021 IEEE 93rd Vehicular Technology Conference (VTC2021-Spring)*, 1-6, doi: 10.1109/VTC2021-pring51267.2021.9448698.

Shrit, O., Martin, S., Al Agha, K. and Pujolle, G. (2018). A New Approach to Realize Drone Swarm Using Ad-Hoc Network. *16th Annual Mediterranean Ad Hoc Networking Workshop (Med-Hoc- Net),* 10.1109/MedHocNet.2017.8001645. hal-01696735

Shukla, A., Xiaoqian, H. and Karki, H. (2016). Autonomous Tracking and Navigation Controller for an Unmanned Aerial Vehicle Based on Visual Data for Inspection of Oil and Gas Pipelines. *16th International Conference on Control, Automation and Systems*.

Ullah, S. *et al*., (2022). Position-Monitoring-Based Hybrid Routing Protocol for 3D UAV-Based Networks. *Drones*, 6(11), 327, doi: 10.3390/drones6110327

Yang H. and Liu Z. (2019). An Optimization Routing Protocol for FANETs. *EURASIP Journal on Wireless Communications and Networking*. Doi: 10.1186/s13638-019-1442-0.

Corresponding author: Emmanuel K. Akut
✉ *akute@unijos.edu.ng*
Department of Electrical and Electronics Engineering, University of Jos.